Version 1.2

MOLA II Laser Transmitter Calibration and Performance

Robert S. Afzal
NASA-GSFC
Laser Remote Sensing Branch
9/19/97

Abstract

The goal of the document is to explain the algorithm for determining the laser output energy from the telemetry data within the return packets from MOLA II. A simple algorithm is developed to convert the raw start detector data into laser energy, measured in millijoules. This conversion is dependent on three variables, start detector counts, array heat sink temperature and start detector temperature. All these values are contained within the return packets. The conversion is applied to the GSFC Thermal Vacuum data as well as the in-space data to date and shows good correlation.

Version 1.2

MOLA II Laser Transmitter Calibration and Performance

Robert S. Afzal
NASA-GSFC
Laser Remote Sensing Branch
9/11/97

Background:

The out going laser energy from the MOLA II laser transmitter is determined from the laser start detector (SD) signal. This is the detector that also starts the instrument's timing clock. When the laser pulse leaves the transmitter there is a fiber optic that collects some scattered light off the turning penta prism (figure 1). The light from the fiber is routed to a detector that integrates the optical signal. The output is a value (number between 0 and 256) proportional to the light energy.
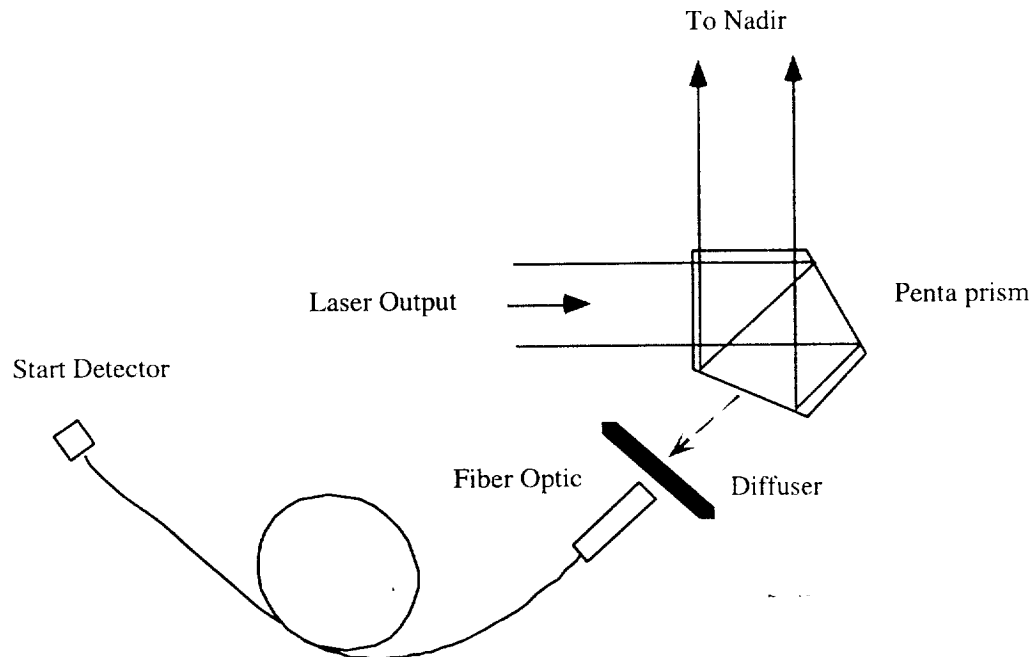

Figure 1

Ideally, this proportionality is linear and a fixed relationship or "factor" would immediately translate Start Detector (SD) Counts into millijoules (mJ) of laser energy. In practice however, this relationship is a function of the vacuum environment, the laser temperature and the start detector temperature. The goal therefore, is to produce a simple algorithm to convert SD Counts into mJ. All the data used in this document is from only a few relevant data sets. The first is the laser vacuum testing data collected at McDonnell-Douglas, and the rest is from the instrument thermal vacuum (TVAC) testing at GSFC and a laser SD calibration test performed on 4/24/96.

Vacuum

Figure 2 show the laser pulse energy as a function of temperature in vacuum. This data was acquired at McDonnell-Douglas during laser TVAC testing. The laser cavity itself was never again exposed to vacuum until launch and operation in space. When the laser emits a pulse, a small amount ($\approx$ 0.02%) of light transmitted by the penta prim strikes a ground glass diffuser. This scattered light is collected by the fiber optic and represents the optical signal to the SD. The amount of transmitted light from the penta is different in vacuum than it is in air. This is most likely due to the release of absorbed water-vapor from the penta-prism's thin film dielectric coatings. With the loss of water vapor in vacuum, the multi-layer thin film changes reflectivity slightly. The in-vacuum signal is 77.03% of the signal observed in air. That is, for 50 mJ striking the penta, the start detector signal level in vacuum (i.e. Space) will be 77.03% of the signal in air. Therefore we multiply our in air calibration test data (SD Counts) by 0.7703 to correct for the change in penta transmission from air to vacuum. This conversion was determined by comparing SD counts from the 4/24/96 calibration run to the GSFC TVAC counts for a fixed laser temperature.
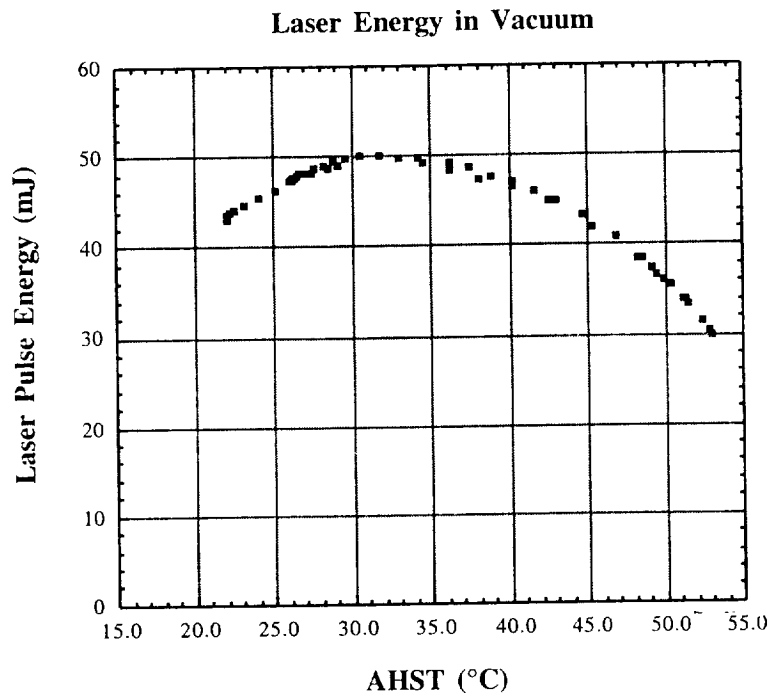
Laser Energy in Vacuum

Figure 2 - Laser pulse energy as a function of diode pump array heat sink temperature (AHST)

4/24/96 Start Detector Calibration

The "4/24/96 Cal." data represents the calibration of the start detector counts, at a fixed start detector temperature, compared to the true laser pulse energy as determined by our Scientec laser power meter. Figure 3 shows SD counts and laser pulse energy, between 20 and 40 °C of the diode array heat sink temperature (AHST), with the start detector fixed at 47 °C. By comparing the data from figure 2 and 3 is can be seen that the laser emits the

same energy in vacuum as is does in air. The task is then only to understand the measurement of the energy and not a change in the energy itself.

Pulse Energy and Start Detector Counts
SD Temp. = 47 °C
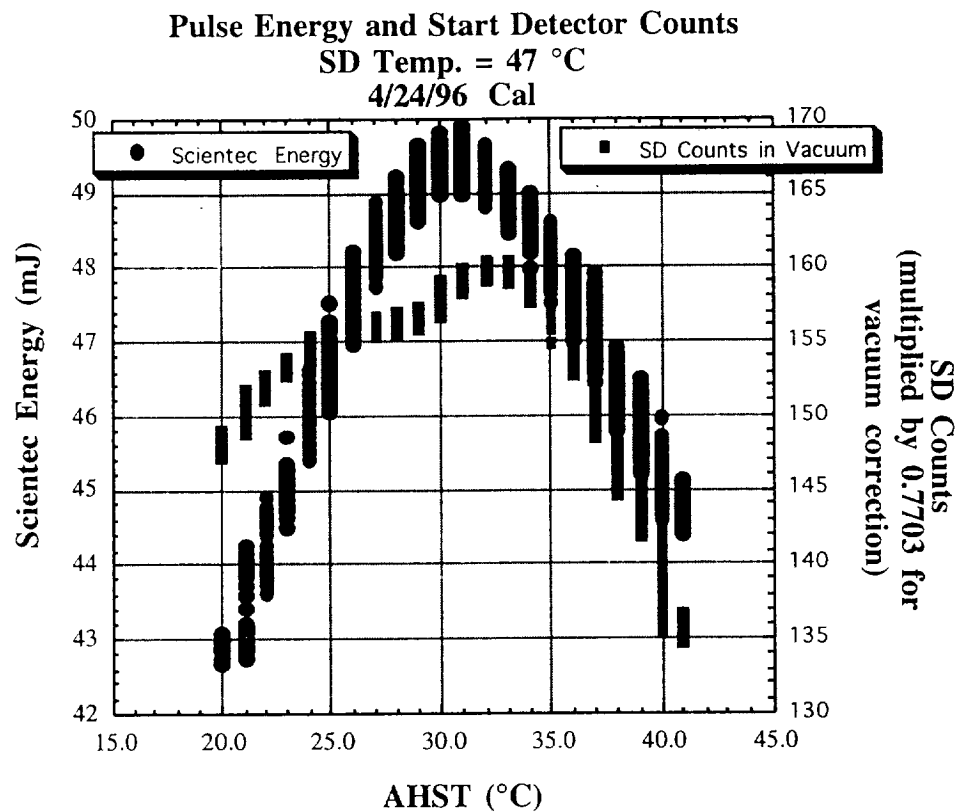**4/24/96 Cal**

Figure 3 - Comparison of the laser pulse energy and corresponding start detector counts.

The relationship between SD counts and laser energy is a function of array heat sink temperature. We divide SD counts by mJ over these temperatures to arrive at a temperature dependent conversion factor (F_{AHST}). See figure 4. A 7th-order polynomial is fitted to the data to generate a smooth function that converts SD counts into mJ. The polynomial coefficients are shown in the window of the figure 3 graph. This curve is only valid between AHST's from 20 to 40 °C.
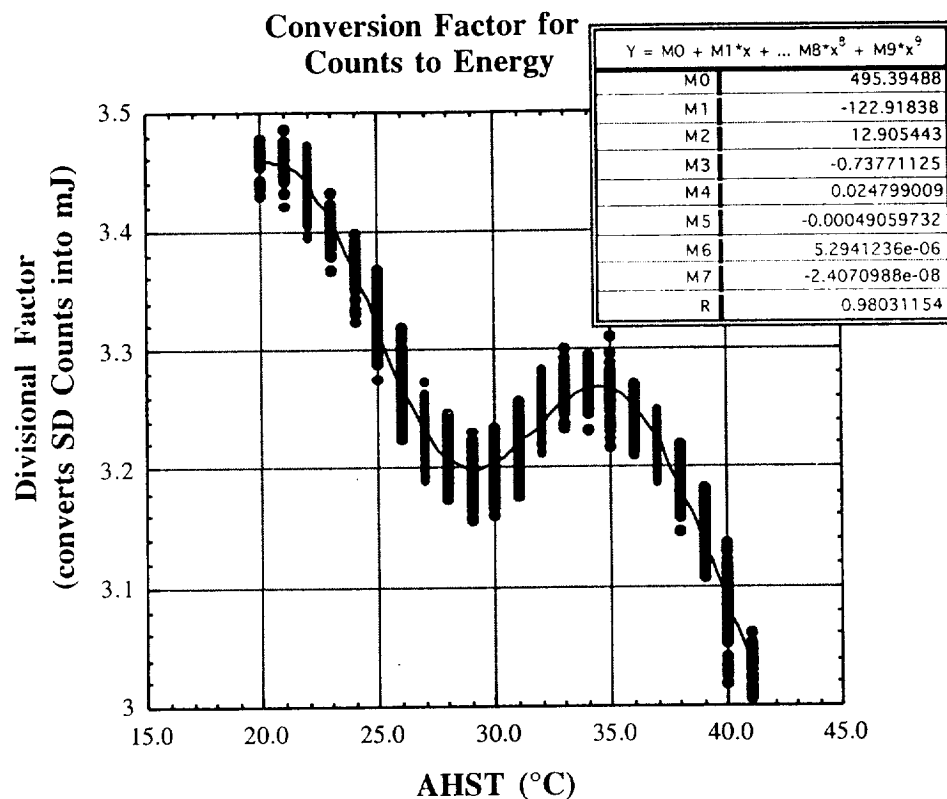
Y = M0 + M1*x + ... M8*x^8 + M9*x^9	
M0	495.39488
M1	-122.91838
M2	12.905443
M3	-0.73771125
M4	0.024799009
M5	-0.00049059732
M6	5.2941236e-06
M7	-2.4070988e-08
R	0.98031154

Conversion Factor for Counts to Energy

Divisional Factor (converts SD Counts into mJ)

AHST (°C)

Figure 4

$$\text{The function } F_{AHST} = 7^{th}\text{-order polynomial(AHST).}$$

We now have the relationship that:

$$\text{Laser Energy} = E_L = (SD \ Counts)/F_{AHST}$$

Start Detector Temperature

The previous relationship for laser energy is valid for the start detector at 47 °C. The start detector responsivity is also a function of its temperature. For higher start detector temperatures the same laser energy will produce higher counts. To normalize the SD Counts for SD Temperature, using the GSFC TVAC data set (Excel file 5_96sd.xls), we graph the response of the SD at fixed laser energy for different SD temperatures. Figure 5 shows this relationship with the laser AHST was at 30 °C, the laser energy peak. Using a linear fit we generate the correction, or "normalization" of the start detector response in relation to our calibrations with the SD at 47 °C. This response is actually only linear and valid over temperatures from about 46 to 53 °C. In addition, depending on laser temperature (or perhaps E-box), the response of the start detector with its temperature is different. A further refinement will be to determine the response of the start detector not only as a

function of temperature but also as a function of AHST (or E-box) temperature and incorporate it into the calibration.
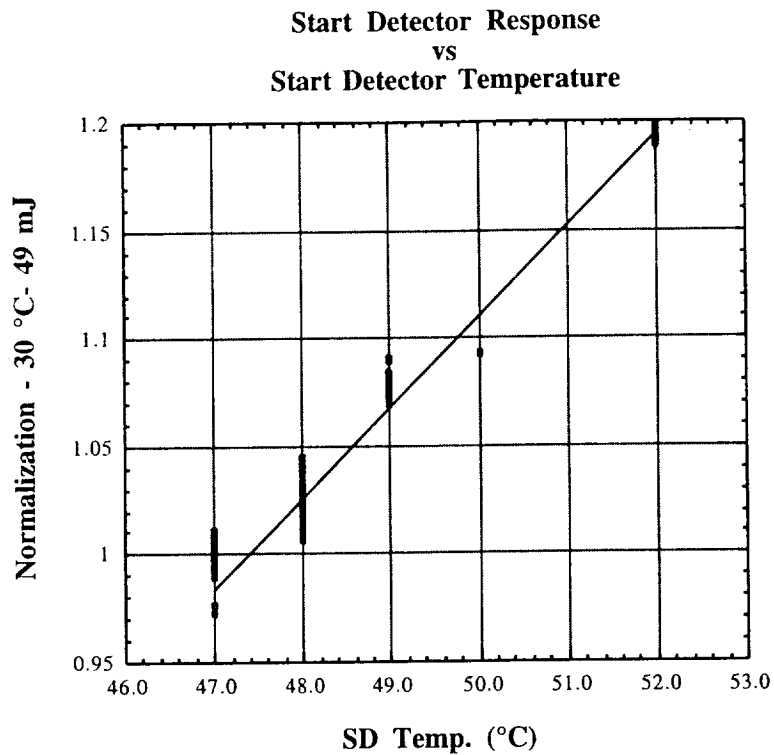
**Start Detector Response
vs
Start Detector Temperature**

Figure 5 - Normalization of start detector response vs. temperature for AHST = 30 °C.

The curve fit is given by:

$$\text{——} \quad y = -1.0032 + 0.042279x \quad R= 0.96281$$

$y = F_{SD}$ = normalization for start detector temperature.

We now have the form:

Laser Energy: $\quad E_L = (SD\ Counts)/(F_{AHST} \cdot F_{SD})$

This allows us to calculate the laser pulse energy given the three variables of SD Counts, AHST and SD Temperature in one equation. As a test of this algorithm, we apply this correction to all the raw GSFC instrument TVAC data. Figure 6 shows the raw, uncorrected data. Figure 7 shows the same data now corrected and overlaid with the thermal vacuum data collected at McDonnell-Douglas in this temperature regime.
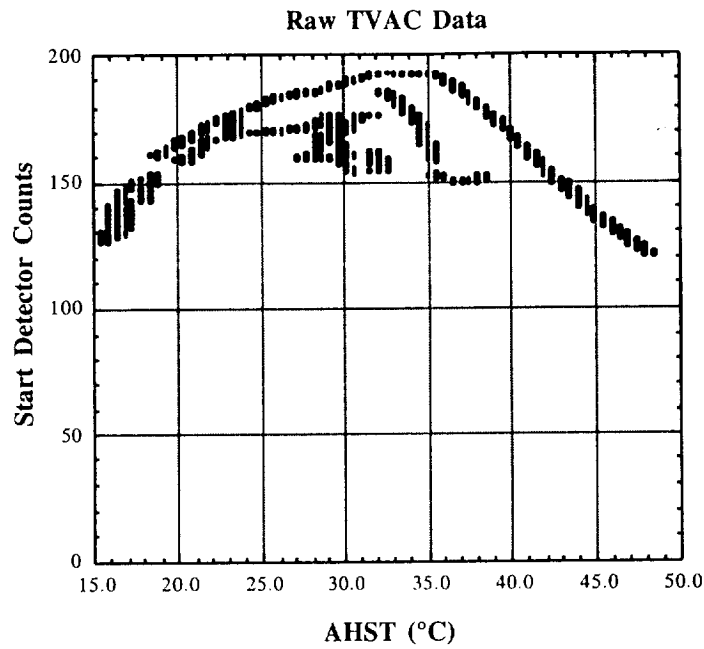
Raw TVAC Data

Figure 6 - Raw start detector counts under all operating conditions during GSFC-TVAC.
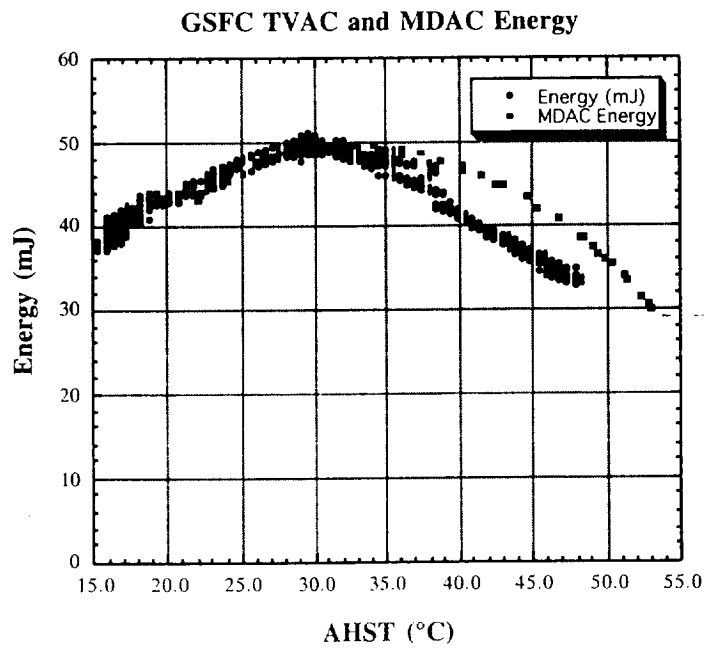
GSFC TVAC and MDAC Energy

Figure 7 - Calibrated fiber pick-off and laser energy.

Notice that the correction is best around where we've used the normalization for the start detector temperature with the laser (AHST) at 30 °C. The linear correction over compensates at higher temperatures and not enough at lower temperatures. Overall though, the start detector has a ± 1 mJ uncertainty shot-to-shot, with up to an estimated ± 5 mJ absolute accuracy depending on the AHST.

We now apply this algorithm to all the in-space operation data, acquired to date, displayed as before in figure 8. This data includes the three in-cruise turn on tests as well as the pass #3, 10 hour planetary encounter as well as the TVAC data acquired at McDonnell-Douglas.
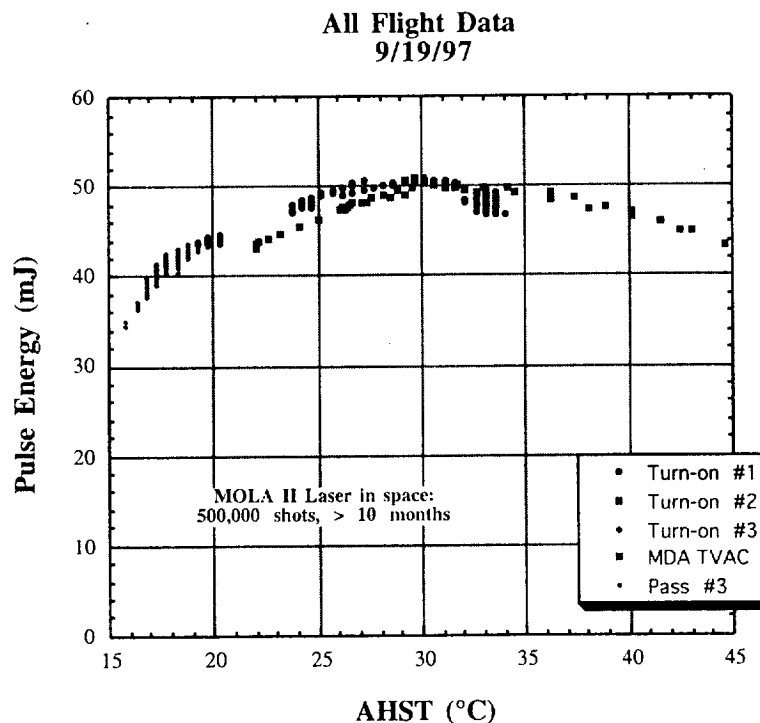
All Flight Data
9/19/97

Figure 8 - Summary of all in-space operation to date compared to TVAC testing.

The in-space data correlates extremely well to the prelaunch TVAC data and, at this point, the laser shows no sign of degradation or change in performance.

Laser Pulse-Width Determination

The transmitted laser pulse width varies as a function of AHST. This is due to the variability of the laser slab gain as the diode laser pumps shift in spectral band as the heat sink temperature changes. The only actual pulse width data we have is at full laser energy (50 mJ) and $T_{pulse} \approx 8$ ns. We can predict the laser pulse-width as a function of pulse energy using numerical modeling. Details of the laser model can be found in reference 1. Figure 9 shows the calculated pulse-width as a function of laser energy.

The data is fitted by a power curve of the form:

$$T_{pulse} = M_0 * X^{M1}$$

Where: T_{pulse} = Pulse-width in nanoseconds
M_0, M_1 are fit constants
X = Laser Energy in millijoules.

Modeled Pulse Width vs Energy

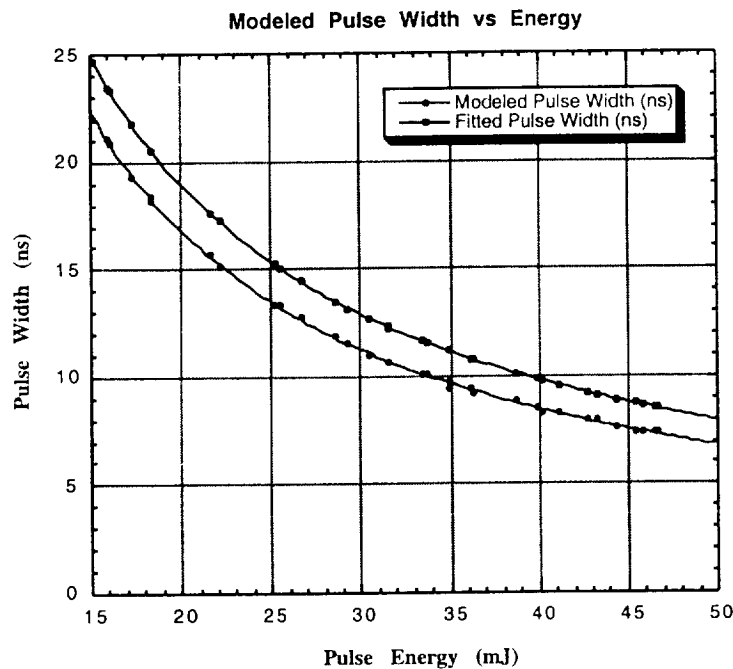

Figure 9 - Modeled relationship between laser transmitted pulse width and energy.

The red curve is a best fit to the modeled data with M0 = 326.62, M1 = - 0.99. Our model tends to predict a slightly shorter pulse-width than is actually measured so we adjust the fit coefficients to match the one data point we have. The blue curve shows a refitted curve adjusting for the laser pulse-width at full energy ≈ 8 ns with M0 = 326.62, M1 = - 0.95.

Conclusion

We are able to measure and determine the MOLA II laser transmitter output pulse energy, as designed, using the start detector fiber optic pick off. The algorithm is fairly simple and depends on three variables, AHST, SD Counts and SD Temperature. Furthermore, the data suggests that the laser did not degrade in performance throughout TVAC testing or operation in space during the transit to Mars.

References

1) R. S. Afzal, "The Mars Observer Laser Altimeter: Laser Transmitter" *Applied Optics* Vol. 33, No. 15, p.3184, 20 May 1994